Journal of Neurochemistry

JOURNAL OF NEUROCHEMISTRY | 2012 | 121 | 996–1006

doi: 10.1111/j.1471-4159.2012.07750.x

ORIGINAL ARTICLE

Modulation of gene expression during early stages of reconnection of the turtle spinal cord

Gabriela García,* Gabriela Libisch,† Omar Trujillo-Cenóz,* Carlos Robello†,‡ and Raúl E. Russo*

*Neurofisiología Celular y Molecular. Instituto de Investigaciones Biológicas Clemente Estable, Montevideo, Uruguay

†Unidad de Biología Molecular, Institut Pasteur de Montevideo, Montevideo, Uruguay

‡Departamento de Bioquímica, Facultad de Medicina, Montevideo, Uruguay

Abstract

The spinal cord of the freshwater turtle *Trachemys dorbignyi* regenerates after complete transection (Rehermann *et al. J. Comp. Neurol.* 515, 2009, 197–214). This remarkable ability may be related to the persistence around the central canal (CC) of progenitors functionally clustered via connexin 43 (Cx43) that express brain lipid binding protein (BLBP) and the transcription factor Pax6 (Russo *et al. J. Neurosci.* 28, 2008, 8510–8516). Indeed, because BLBP+ cells appear in the bridge joining the rostral and caudal stumps, we speculated that progenitors contacting the central canal may play a key part in spinal cord regeneration. To test this hypothesis, we designed degenerated primers pairing conserved regions for key proteins synthesized in progenitors (BLBP, Cx43, and Pax6) and the neuronal protein HuB. Fragments of these proteins were amplified, cloned, and sequenced. Based on these sequences, we analyzed the changes in the expression levels using quantitative real-time RT-PCR with specific primers, comparing the injured spinal cord at different times after injury (4, 12, 20, and 60 days) with uninjured spinal cords. We found a transient, early increase of BLBP, Cx43 and HuB mRNA, with Pax6 remaining unchanged. These results suggest that the selected genes – active in progenitor cells – play an important part in early mechanisms of spinal cord regeneration.

Keywords: BLBP, connexin 43, Pax6, quantitative real-time PCR, regeneration, spinal cord.

J. Neurochem. (2012) **121**, 996–1006.

In mammals, spinal cord injury results in gliosis and limited cellular regeneration, leading to devastating conditions (Thuret *et al.* 2006). In contrast, larval cyclostomes, some teleosts, and tailed amphibians keep substantial endogenous repair capabilities with restoration of locomotion after injury (Tanaka and Ferretti 2009). It is generally accepted that urodeles are the most evolved vertebrates with a robust regenerative potential of the adult spinal cord (Stensaas, 1983). However, we have shown (Rehermann *et al.* 2009) that freshwater turtles are able to reconnect their transected spinal cords, leading to some degree of recovery of motor functions. In contrast to mammals, no glial scar is observed in turtles but instead regenerating axons cross the injured site approximately 20 days after the lesion. These regenerating axons travel on a scaffold formed by newly generated glial cells that express the brain lipid binding protein (BLBP) and/or the glial fibrillary acidic protein (GFAP) (Rehermann *et al.* 2009, 2011).

The endogenous repair of the spinal cord in turtles may be linked to the existence of domains of progenitor cells lining the central canal (CC). These cells exhibit proliferative capacity, are coupled via connexin 43 (Cx43), and express both BLBP and the transcription factor Pax6 (Russo *et al.* 2008). It is believed that connexins play an important role in the regulation of proliferation, migration, and cell differentiation (Bruzzone and Dermietzel 2006). In particular, Cx43 appears essential for maintaining neural progenitors in a proliferative state (Duval *et al.* 2002; Cheng *et al.* 2004). BLBP is a member of the large family of hydrophobic ligand-binding proteins that modulate transcription through their interactions with nuclear receptors (Haunerland and Spener 2004) and is required to induce

Received January 26, 2012; revised manuscript received March 16, 2012; accepted March 21, 2012.

Address correspondence and reprint requests to Dr. Raúl E. Russo, Departamento de Neurofisiología Celular y Molecular, Instituto de Investigaciones Biológicas, Clemente Estable, Avenida Italia 3318, CP 11600, Montevideo, Uruguay. E-mail: rrusso@iibce.edu.uy

Abbreviations used: BLBP, brain lipid binding protein; CC, central canal; Cx43, connexin 43; GFAP, glial fibrillary acidic protein; LDH, lactate dehydrogenase; PB, phosphate buffer; PK, pyruvate kinase; RG, radial glial.

morphological changes in radial glial (RG) in response to neuronal cues (Feng *et al.* 1994; Anton *et al.* 1997). Finally, the transcription factor Pax6 is expressed in RG lining the ventricle cavities and is an important regulator of the neurogenic capabilities of progenitors during development (Heins *et al.* 2002; Pinto and Götz 2007) and in neurogenic niches of the adult brain (Kohwi *et al.* 2005). In the spinal cord, Pax6 is part of the transcriptional code that determines subsets of progenitors giving rise to specific neuronal types (Lee and Pfaff 2001), controlling the tempo of neuronal differentiation (Bel-Vialar *et al.* 2007).

Because the persistence of CC-contacting progenitors may be one of the central features supporting the outstanding regeneration capability in turtles (Rehermann *et al.* 2009, 2011), we hypothesized that spinal cord injury may trigger changes in the expression of key genes that drive protein synthesis in these cells. To test this idea, we selected the BLBP, Pax6, and Cx43 genes expressed in CC-contacting progenitors and HuB, a gene active from the earliest stages of neuronal differentiation (Marusich *et al.* 1994). Because there is no information about the sequence of these genes in turtles, we first designed degenerate oligonucleotides priming conserved regions of the genes, together with specific primers for the putative control genes pyruvate kinase (PK) and lactate dehydrogenase (LDH). We next amplified fragments of these genes, cloned, and sequenced them. Based on these data, we analyzed the changes in mRNA expression levels using real-time RT-PCR with specific primers, comparing injured segments (T10-11) with their counterparts in control animals at different time points after spinal cord transection. To analyze the spatial profile of the change in gene expression, we performed immunohistochemistry in injured and normal animals. Our results revealed significant increments in the expression of BLBP, Cx43, and HuB genes 4 days after injury while Pax6 remained unchanged at the same time point. However, BLBP and Cx43 returned to normal values around day 12, a time point when anatomical reconnection is still incipient (Rehermann *et al.* 2009). Conversely, Hu remained underexpressed at 12, 20, and 60 days post injury. The immunohistochemical data showed that the spatial profile of expression of these genes was conserved in spinal cord stumps. Our findings suggest that modulation of BLBP and Cx43 gene expression is transiently involved in the early plasticity triggered by spinal cord injury. It remains to be clarified whether this early response is instrumental for later stages of post-transcriptional mechanisms commanding endogenous neural repair.

Methods

Animals

Fresh-water turtles (*Trachemys dorbignyi*, 5–12 cm carapace length) were used (n = 22). These juvenile turtles (2 months to 1 year old) behave like fully mature animals in terms of their sensory-motor behavior. The animals were maintained in temperate aquaria (24–26°C) under natural illumination and fed daily with small earthworms. The ARRIVE guidelines have been followed, and all experimental procedures were performed in accordance with the ethical guidelines established by our local Committee for Animal Care and Research at the Instituto de Investigaciones Biológicas Clemente Estable. Every precaution was taken to minimize animal stress and the number of animals used.

Surgical procedures

The detailed surgical procedures to lesion the spinal cord have been described elsewhere (Rehermann *et al.* 2009). Briefly, animals were sedated by intraperitoneal injection of ketamine chlorhydrate (40 mg/kg b.w.). Then, the legs were secured to a rigid support by means of rubber bands, and complete anesthesia was achieved by inhalation of isofluorane (1-chloro-2,2,2-trifluoroethyl difluoromethyl ether; Forane, Abbot Laboratories, Berkshire, UK). To prevent infection, we rubbed the carapace with a cotton pad previously immersed in an alcohol-iodine solution, and all surgical instruments were sterilized by using chemical procedures. After the animal was unresponsive to nociceptive stimuli, we opened a window in the carapace following the limits of the third dorsal scute to expose the spinal cord. Complete transection of the spinal cord (T10-11) was performed with a thin-blade scalpel. After washing the injured site with sterile saline, we replaced the lifted scute and sealed the injured carapace with cyanoacrylate adhesive.

Post-operative care

We identified spinalized turtles with indelible marks sculptured on their carapace. Turtles do not require special post-operative care because, as described for other non-mammalian vertebrates (Mountcastle 1980), spinal shock is very short. Because turtles have a primitive ''allantoic bladder'' opening into the cloaca (Parker and Harwell 1949), there is no noticeable urine retention. Despite their reduced motor capabilities, injured turtles were able to catch living worms a few days after surgery.

Tissue preparation

For the cloning and sequencing of the genes of interest, the whole spinal cords (n = 3) were rapidly removed and placed in RNAlater (Sigma) for storage at −80°C. For quantitative real-time PCR analysis, we studied a total of 12 turtles that were examined using the following protocol: three turtles were killed 4 days after surgery; three turtles were killed 12 days after surgery; three turtles were killed 20 days after surgery; three turtles were killed 60 days after surgery. In all cases, a 4-mm long spinal cord segment centered on the lesion epicenter was quickly dissected out, placed in RNAlater (Sigma-Aldrich, St. Louis, MO, USA), and stored at −80°C. The corresponding spinal cord segments of control-uninjured and sham-injured animals were processed in the same way.

RNA extraction and reverse transcription

The tissue was mechanically homogenized using a Cordless motor and pellet pestle (Sigma-Aldrich). Total RNA from the spinal cord was extracted and purified using TRIZOL reagent (Invitrogen, Carlsbad, CA, USA) following the manufacturer's protocol. The concentrations of RNA samples were quantified using the Nanodrop (Nano-Drop Inc., Rockland, DE, USA). RNA integrity was determined using Bioanalyzer (Agilent Technologies, Santa Clara,

Table 1. Sequence of degenerated and specific primer pairs used for RT-PCR

	Sequence 5′-3′	Fragment size (bp)
Connexin 43		
Forward primer	GARCAYGGNAARGTNAARATG	495
Reverse primer	RTARTTNGCCCARTTYTGYC	
BLBP		
Forward primer	RTARTTNGCCCARTTYTGYTC	240
Reverse primer	NARNGTCATNACCAT	
HuB		
Forward primer	ATGACNATHGAYGGNATG	240
Reverse primer	GARATGCARCARATGGCNWSN	
PAX6		
Forward primer	ATGGGNGCNGAYGGNATGTAY	750
Reverse primer	RTTCATRTGNGTYTGCATRTG	
LDH GenBank accession Number: L79954.1		
Forward primer	GGCCAAGTTGGAATGGCCTGTG	439
Reverse primer	GCCATCAGATGGCGAAATCTAGC	
PK GenBank accession Number: AJ243137.1		
Forward primer	GATGGGCTCATCTCCCCTGCTGG	432
Reverse primer	TTCCCGGCACGGTTGCAG	

CA, USA), and only samples with a RNA Integrity Number (RIN) higher than 7 were used for reverse transcription (Figure S1). For spinal cord segments of injured and uninjured animals, cDNA synthesis was performed using the same amount of starting RNA (0.5 μg). The enzyme Superscript III was used (Invitrogen) primed with oligo(dT) according to the manufacturer's instructions.

Cloning and sequencing

Degenerated and specific primers were designed to hybridize highly conserved regions of the genes of interest coding sequences (Table 1). The PCR products amplified from spinal cord cDNA were analyzed by agarose gel electrophoresis. When needed, gel purification was performed with the kit GenElute gel extraction kit (Sigma-Aldrich). PCR products were cloned using the pGEMT Easy Vector System (Promega, Madison, WI, USA). Colonies were selected and plasmids purified from 3 ml of liquid media LB. Inserts were sequenced with Sp6 and T7 universal primers using an ABI3130 (Applied Biosystems, Foster City, CA, USA) DNA automatic sequencer. Sequences from multiple clones were aligned to generate consensus sequences, which were then used in nucleotide basic local alignment search tool (BLAST) searches to retrieve orthologous ones.

Alignment of amplified gene fragments with orthologs from other vertebrates was done online with ClustalW2 (http://www.ebi.ac.uk/Tools/msa/clustalw2/). We used the online ExPASy tool (http://ca.expasy.org/tools/dna.html) for *in silico* translation of nucleotide sequences to examine conservation at the amino acid level.

Quantitative Real-time PCR Analysis

Four-millimeter long segments of spinal cord centered on the lesion epicenter were compared with corresponding segments of control animals. Injured animals (n = 3 for each time point) were killed at different times post injury (4, 12, 20, and 60 days). With the cloned sequences, specific primers were designed for amplifying small fragments (~ 200 pb, Table 2). Using a real-time cycler Rotor Gene 6000 (Corbett Research, Bath, UK) and SYBR Green I, the genes of interest were amplified. Briefly, each reaction tube contained 5 μL of 2X SYBR Green Quantimix solution (Biotools), 250 nM of each forward and reverse primer, 0.5 μL of cDNA and water to bring the total reaction volume to 10 μL. The thermal profile was 95°C for 5 min followed by 40 cycles of three steps (95°C for 15 s, 55°C for 20 s, and 72°C for 20 s). The PCR for each cDNA sample and plasmid DNA standard was performed in duplicate.

Table 2. Sequence of primer pairs used for real-time RT-PCR

	Sequence 5′-3′	Fragment size (bp)
Connexin 43		
Forward primer	TGGTACGTCTATGGGTTTAGC	214
Reverse primer	CTGGTTTTCCTTTCACACGA	
PAX6		
Forward primer	AGAGCAAATTGAAGCCCTTG	238
Reverse primer	TGGTTGGTAGACACTTGTGC	
BLBP		
Forward primer	AGGGCGACAAGGTCACTGTGA	171
Reverse primer	TGCCGTCCCATTTCTGCACA	
HuB		
Forward primer	CCAGTTTGGCCGGAATTAATATC	155
Reverse primer	AGTCACGGATGACCTTCACGTTG	
GFAP		
Forward primer	GCCAGTTACATCGAGAAGGT	554
Reverse primer	GTCAGGTCTGCAAACTTGGA	

Control reactions were performed to verify the absence of genomic DNA and cross contamination of any other DNA source. A melting temperature analysis was added at the end of each real-time PCR to verify that a single product was amplified for each gene analyzed.

Standard curve construction

Because the intended housekeeping genes LDH and PK changed dramatically following spinal cord transection (data not shown), we used an absolute transcript quantification method. The plasmidic vectors pGEM-T easy (Promega) containing the sequences of interest used previously were also used for the construction of the standard curves which were based on real-time PCR of known quantities of plasmidic DNA. Each standard curve was generated based on five 10-fold serial dilutions of a starting concentration of DNA (100 pg/μL) converted to the number of copies using the molecular mass of the DNA: Attomoles (amoles) of input plasmid DNA = 1.52 × amount of input plasmid DNA/plasmid length, according to Wu *et al.* (2005). A standard curve plotting CT values against the logarithm of input DNA copy quantity (log amoles) was constructed for each gene. The number of copies in the experimental samples was calculated from the equation of the line for the standard curve.

Data analysis

Standard DNAs, negative controls, and cDNA obtained from uninjured animals and samples obtained at different times after injury (4, 12, 20, and 60 days) were run simultaneously for each of

the genes analyzed. The data for the uninjured controls were presented as amole/μg RNA ± SEM, and the relative gene expression data for the different times after injury were expressed as the ratio to the amole/μg RNA of the sample divided by the same value in the control. Statistical significance was evaluated with the unpaired *t*-test at $p < 0.05$.

Immunohistochemistry

The spinal cords of anesthetized turtles (50 mg/kg pentobarbital) were fixed by intracardiac perfusion. For immunohistochemistry ($n = 6$ animals), we used 10% paraformaldehyde dissolved in 0.1 M phosphate buffer (PB; pH 7.4). Fixed material was sectioned in the transverse plane (60–80 μm) with a vibrating-blade microtome. We used the following primary antibodies: (i) anti-BLBP (rabbit polyclonal, 1:1000; Chemicon International Inc., Temecula, CA); (ii) anti-HuC/D (mouse monoclonal, 1:50; Molecular Probes, Eugene, OR), (iii) anti-Cx43 (rabbit polyclonal, 1:3000; kindly provided by Dr. J.C. Saez; PUC University, Santiago, Chile), and (iv) anti-GFAP (mouse monoclonal, 1:500, Sigma). Non-specific reactive sites were blocked with 0.5% bovine serum albumin in PB (1 h) followed by overnight incubation with the primary antibody in PB containing 0.3% Triton X-100. After blocking and washing, the tissues were incubated with goat anti-rabbit or goat anti-mouse secondary antibodies conjugated with Alexa 488 (1:1.000, 2 h; Invitrogen, Eugene, OR, USA). Finally, the sections were thoroughly washed and mounted. Control experiments replacing antibodies with pre-immune serum and negative controls without primary antibodies were routinely performed.

Since Cx43 immunohistochemistry revealed a dotted pattern, it was possible to use an automatic counting procedure. The number of punctae was quantified from four confocal optical sections of control animals and turtles with the transected spinal cord at 4 and 12 days post injury (DPI). For this purpose, we used the command Analyze particles of ImageJ (available at http://rsbweb.nih.gov/ij/), after setting appropriately the threshold level.

Results

Cloning and sequencing

Because the complete genome of any chelonian has not been sequenced yet, there is no genetic information available for performing a BLAST analysis or for the design of specific primers. To overcome this limitation, we did multiple alignments of the sequences of interest (PAX6, Cx43, Hu protein and BLBP) and designed degenerated primers of highly conserved regions. For the fragments of housekeeping genes (LDH and PK), we designed specific primers based on sequences from *Trachemys scripta* (Table 1). With these primers, PCR was performed with cDNA under conditions optimized for each gene obtaining amplified PCR fragments of the expected size (Fig. 1).

The PCR products were then purified and cloned in the pGEM-T vector, and multiple clones were sequenced and aligned to generate consensus sequences, which were then used in nucleotide BLAST searches to retrieve orthologous genes. The deduced aminoacidic sequences were aligned

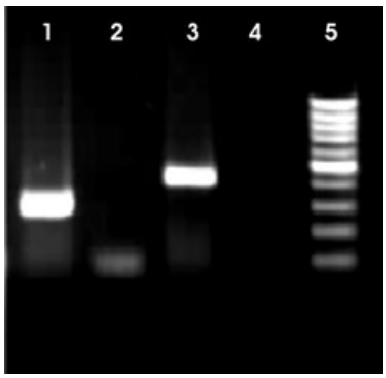

Fig. 1 Gel electrophoresis of PCR products from turtle spinal cord cDNA. A single band was detected near the expected size in bp for each target gene. No band was observed in the PCR products of negative controls. Lane 1, BLBP, expected size 240 pb; lane 2, negative control without cDNA; lane 3, Cx43, expected size 495 pb; lane 4, negative control without cDNA; and lane 5, molecular weight marker.

with orthologs from other organisms from different taxa. Interestingly, all the cloned genes exhibited a very high degree of conservation at the aminoacidic level. HuB displayed the highest level of conservation (Fig. 2): 100% when compared with a bird (*Gallus gallus*), 98% with two mammals (*Mus musculus* and *Homo sapiens*) and an amphibian (*Xenopus laevis*). PAX6 also presented a very high level of conservation, being more than 93%when compared with birds (*Columba livia* and *G. gallus*), mammals (*Rattus norvergicus* and *H. sapiens*), and amphibians (*X. laevis*) (Fig. 3). Moreover, Cx43 of *T. dorbignyi* exhibited an identity higher than 77% when compared with *G. gallus, M. musculus, H. sapiens,* and *Danio rerio* (Fig. 4). Finally for BLBP, the identity level was 76% with *Salmo salar*, 73% with *G. gallus,* 71% with *X. laevis,* 69% with *H. sapiens,* and 65% with *R. norvergicus* (Fig. 5).

LDH and PK also displayed high conservation degrees when compared with other organisms (data not shown, accession numbers: JQ356536 and JQ356537, respectively).

Standard curves for quantification and identification of the amplicons

The standard curves for the genes of interest were appropriate for quantitative analyses (Figure S2). The average slope of the Ct versus initial template plots was −3.39 ± 0.05 SD and the mean of the efficiency was 97 ± 2% SD ($n = 5$). These values were similar to the predicted ones (slope and efficiency for the 10-fold dilutions, −3.3 and 100%), being the average correlation (r^2) of all the standard curves 0.993 ± 0.004. The melting curve analysis for each target gene showed a unique peak not observed in the corresponding negative control.

Gel electrophoresis of real-time PCR products is shown in Fig. 6. A single band was detected at the expected size for each target gene, whereas no band was observed in the

```
T. dorbignyi    ---------------------------MTSLAGINIPGHAGTGWCIFVYNLAPDADESIL 33
Gallus gallus   QAQRFRLDNLLNMAYGVKRFPPMTIDGMTSLAGINIPGHAGTGWCIFVYNLAPDADESIL 295
Mus musculus    QAQRF------------SRFSPMTIDGMTSLAGINIPGHPGTGWCIFVYNLAPDADESIL 280
Homo sapiens    QAQRFRLDNLLNMAYGVKRFSPMTIDGMTSLAGINIPGHPGTGWCIFVYNLAPDADESIL 300
X. Tropicalis   QAQRF------------SRFSPMTIDGMTSLAGINFPGHAGTGWCIFVYNLAPDADESIL 279
                                        ********:***.********************

T. dorbignyi    WQMFGPFGAVTNVKVIRDFNTNKCKGFGFVTMTNYDEA---------------------- 71
Gallus gallus   WQMFGPFGAVTNVKVIRDFNTNKCKGFGFVTMTNYDEAAMAIASLNGYRLGDRVLQVSFK 355
Mus musculus    WQMFGPFGAVTNVKVIRDFNTNKCKGFGFVTMTNYDEAAMAIASLNGYRLGDRVLQVSFK 340
Homo sapiens    WQMFGPFGAVTNVKVIRDFNTNKCKGFGFVTMTNYDEAAMAIASLNGYRLGDRVLQVSFK 360
X. Tropicalis   WQMFGPFGAVTNVKVIRDFNTNKCKGFGFVTMTNYDEAAMAIASLNGYRLGDRVLQVSFK 339
                ************************************
```

Fig. 2 Multiple alignments for the ELAV family protein HuB. The homology between the sequences of *Mus musculus* (NP_997568.1), *Homo sapiens* (BAD92531.1), *Gallus gallus* (XP_001233484.1), *Xenopus tropicalis* (NP_001025498.2), and *Trachemys dorbignyi* (JQ356535) is higher than 98%.

```
Columba         QMGADGMYDKLRMLNGQTGTWGTRPGWYPGTSVPGQPAQDGCPQQEGGGENTNSISSNGE 173
Gallus          QMGADGMYDKLRMLNGQTGTWGTRPGWYPGTSVPGQPAQDGCPQQEGGGENTNSISSNGE 209
Rattus          QMGADGMYDKLRMLNGQTGSWGTRPGWYPGTSVPGQPTQDGCQQQEGQGENTNSISSNGE 209
Homo            QMGADGMYDKLRMLNGQTGSWGTRPGWYPGTSVPGQPTQDGCQQQEGGGENTNSISSNGE 195
Xenopus         QMGSEGMYDKLRMLNGQTATWGSRPGWYPGTSVPGQPAQEGCQPQEGVGENTNSISSNGE 226
Trachemys       ---------------------------------------------KEEVKNTNSISXXGE 15
                                                              :   :******  **

Columba         DSDEAQMRLQLKRKLQRNRTSFTQEQIEALEKEFERTHYPDVFARERLAAKIDLPEARIQ 233
Gallus          DSDEAQMRLQLKRKLQRNRTSFTQEQIEALEKEFERTHYPDVFARERLAAKIDLPEARIQ 269
Rattus          DSDEAQMRLQLKRKLQRNRTSFTQEQIEALEKEFERTHYPDVFARERLAAKIDLPEARIQ 269
Homo            DSDEAQMRLQLKRKLQRNRTSFTQEQIEALEKEFERTHYPDVFARERLAAKIDLPEARIQ 255
Xenopus         DSDEAQMRLQLKRKLQRNRTSFTQEQIEALEKEFERTHYPDVFARERLAAKIDLPEARIQ 286
Trachemys       DSDEAQMRLQLKRKLQRNRTSFTQEQIEALEKEFERTHYXDVFARERLAAKIDLPEARIQ 75
                ************************************ ********************

Columba         VWFSNRRAKWRREEKLRNQRRQASNTPSHIPISSSFSTSVYQPIPQPTTPVSSFTSGSML 293
Gallus          VWFSNRRAKWRREEKLRNQRRQASNTPSHIPISSSFSTSVYQPIPQPTTPVSSFTSGSML 329
Rattus          VWFSNRRAKWRREEKLRNQRRQASNTPSHIPISSSFSTSVYQPIPQPTTPVSSFTSGSML 329
Homo            VWFSNRRAKWRREEKLRNQRRQASNTPSHIPISSSFSTSVYQPIPQPTTPVSSFTSGSML 315
Xenopus         VWFSNRRAKWRREEKLRNQRRQASNTPSHIPISSSFSTSVYQPIPQPTTPVSSFTSGAML 346
Trachemys       VWFSNRRAKWRGEEKLRNQRRQASNTPSHIPISSSFSTSVYQPIPQPTTPVSSFTSGSML 135
                *********** ********************************************:**

Columba         GRTDTALTNTYSALPPMPSFTMANNLPMQPPVPSQTSSYSCMLPTSPSVNGRSYDTYTPP 353
Gallus          GRTDTALTNTYSALPPMPSFTMANNLPMQPPVPSQTSSYSCMLPTSPSVNGRSYDTYTPP 389
Rattus          GRTDTALTNTYSALPPMPSFTMANNLPMQPPVPSQTSSYSCMLPTSPSVNGRSYDTYTPP 389
Homo            GRTDTALTNTYSALPPMPSFTMANNLPMQPPVPSQTSSYSCMLPTSPSVNGRSYDTYTPP 375
Xenopus         GRTDTALTNSYSALPPMPSFTMGNNLPMQPPVPSQTSSYSCMLPTSPSVNGRSYDTYTPP 406
Trachemys       GRTDTALTNTYSALPPMPSFTMANNRPMQPPVPSQTSSYSCMLPTSPSVXGRSYDTYXP- 194
                *********:************.** ********************** ******* *
```

Fig. 3 Multiple alignments of PAX6 aminoacidic sequence. There is a high homology (more than 93%) between species such as *Columba* (ABI98850), *Rattus norvergicus* (ADN04686.1), *Gallus gallus* (NP_990397.1), *Homo sapiens* (NP_000271), *Xenopus laevis* (AAB36681.1), and *Trachemys dorbignyi* deduced aminoacidic sequence (JQ356533).

negative controls. To confirm that the expected genes were amplified, we sequenced the real-time PCR products, obtaining the expected sequences in all cases (data not shown). Thus, each target molecule was amplified and detected with the primer sets used.

Gene expression in the uninjured spinal cord

To analyze the possible changes in expression induced by injury, we first characterized the expression of the genes of interest in the normal spinal cord. We originally examined the expression relative to potential reference genes (LDH, PK), but as they changed dramatically after injury, we chose to express data as amole/μg RNA to reflect actual alterations *in vivo* following a strategy used by Wu *et al.* (2005). Figure 7 shows the absolute quantity of the mRNA for target genes in uninjured spinal cords. Cx43 was the most expressed gene with 244 ± 30 amole/μg RNA. BLBP mRNA was the next most abundant gene product with an expression of 52 ± 6 amole/μg RNA, followed by HuB (21 ± 2 amole/μg RNA). Finally, the mRNA for PAX6 was the least abundant: 11 ± 1 amole/μg RNA.

Changes in gene expression levels after injury

Real-time PCR with specific primers based in our sequences allowed us to identify differences in the expression level of Cx43, HuB, PAX6, and BLBP when compared with control. In each case, the data values were presented as the ratio to the amole/ug RNA of the sample divided by the same value in control (Fig 8). Cx 43 was the gene that showed the highest level of over-expression, being 1.7 ± 0.1 folds ($p < 0.05$) 4 days after injury and decreasing to not significantly different levels in the other time points analyzed. BLBP was over-expressed 1.5 ± 0.1 times relative to control ($p < 0.05$) at 4 days after injury reaching normal levels from day 12. The expression of HuB also peaked at 4 days after injury (1.5 ± 0.1, $p < 0.01$) and significantly decreased below control levels in the next time point studied (0.5 ± 0.2, $p < 0.05$). This down-regulation was unchanged during the rest of the time course analyzed (0.6 ± 0.1 at 20 and 60 days post injury, $p < 0.05$). PAX6 was the only gene that did not change significantly at any time point after injury. Gene expression for the explored genes in sham-injured animals – in which all surgical procedures were

```
Homo        VNVDMHLKQIEIKKFKYGIEEHGKVKMRGGLLRTYIISILFKSIFEVAFLLIQWYIDGFS 180
Mus         VNVEMHLKQIEIKKFKYGIEEHGKVKMRGGLLRTYIISILFKSVFEVAFLLIQWYIYGFS 180
Gallus      VNVDMHLKQIESKKFKYGIEEHGKVKMRGGLLRTYIISILFKSVFEVAFLLIQWYIYGFS 180
Trachemys   ----------------------EHGKVKMRGGLLRTYIIXILFKSVFEVAFLVIQWYVYGFS 40
Danio       GDVELHLKKIELKKFKHGLEEHGKVKMKGSLLRTYIFSIIFKSICEVVFLVIQWYLYGSS 81
                                    *******:*.******: *:***: **.**:****: * *

Homo        LSAVYTCKRDPCPHQVDCFLSRPTEKTIFIIFMLVVSLVSLALNIIELFYVFFKGVKDRV 240
Mus         LSAVYTCKRDPCPHQVDCFLSRPTEKTIFIIFMLVVSLVSLALNIIELFYVFFKGVKDRV 240
Gallus      LSAIYTCERDPCPHRVDCFLSRPTEKTIFIVFMLVVSLVSLALNIIELFYVFFKGVKDRV 240
Trachemys   LNAIYTCERDPCPHRVDCFLSRPTEKTIFIIFMLVVSLVSLALNIIELXYVFFKGVKDRV 100
Danio       LSAVYTCERTPCPHRVDCFLSRPTEKTIFIIFMLVVSLFSLLLNIIELFYVLFKRIKDRV 141
            *.*:***:* ****:***************:*******.** ****** **:** :****

Homo        KGKSDPYHATSGALSPA-KDCGSQKYAYFNGCSSPTAPLSPMSPPGYKLVTGDRNNSSCR 299
Mus         KGRSDPYHATTGPLSPS-KDCGSPKYAYFNGCSSPTAPLSPXXPPGYKLVTGDRNNSSCR 299
Gallus      KGKTDPY-SHSGTMSPS-KDCGSPKYAYYNGCSSPTAPLSPMSPPGYKLVTGDRNNSSCR 298
Trachemys   KGKPDPY-SPTGTVSPA-KECGSTKYAYFNGCSSPTAPLSPMSPPGYKLVTGD------- 151
Danio       KSRQNTQ-FPTGTLSPTPKELSTTKYAYYNGCSSPTAPLSPMSPPGYKLATGERTN-SCR 199
            *.: :.    :*.:**: *: .: ****:************  ******.**:
```

Fig. 4 Multiple alignments for Cx43. The homology between the sequences of *Gallus gallus* (NP_989917), *Homo sapiens* (BAD97009.1), *Danio rerio* (AAH49297.1) and *Mus musculus* (AAA53027.1), and *Trachemys dorbignyi* (JQ356532) is higher than 77%.

```
Homo        MVEAFCATWKLTNSQNFDEYMKALGVGFATRQVGNVTKPTVIISQEGDKVVIRTLSTFKN 60
Rattus      MVDAFCATWKLTDSQNFDEYMKALGVGFATRQVGNVTKPTVIISQEGGKVVIRTQCTFKN 60
Gallus      MVEAFCATWKLADSHNFDEYMKALGVGFAMRQVGNVTKPTVIISSEGDKVVIRTQSTFKN 60
Xenopus     MVDVFCATWKLIDSQNFDEYMKALGVGFATRQVGNVTKPTVIINQEGDKVVIRTQSTFKN 60
Salmo       MVDAFCATWKLVDSDNFDEYMKALGVGFATRQVGNVTKPTVIIAKEGDKVVVKTQSTFKN 60
Trachemys   ------------DX--FDEYMKAIGVXFAMRQIXNLTKPTTTIXLEGDKVTVKTQSTFKS 46
                       :   *******:** ** **: *:****. *  **.**.::* .***.

Homo        TEISFQLGEEFDETTADDRNCKSVVSLDGDKLVHIQKWDGKETNFVREIKDGKMVMTLTF 120
Rattus      TEISFQLGEEFEETSIDDRNCKSVIRLDGDKLIHVQKWDGKETNCVREIKDGKMVVTLTF 120
Gallus      TEISFKLGEEFDETTPDDRNCKSVVTLDGDKLVHVQKWDGKETNFVREIKDGRMVMTLTF 120
Xenopus     TEVSFKLGEEFDEATADDRNCKSTVTLEGDKLVHVQKWDGKETKFVREIKDGKMIMTLTF 120
Salmo       TEISFKLGEEFDEATADDRNCKSTVSLDGDKLAHVQKWDGKEAKFVREIKDGKLVMTLTF 120
Trachemys   TEISFKLGEEFDEMTADDRHVKSLVTLDGGKLIHVQKWDGKX------------------ 88
            **:**:*****:* : ***: ** : *:*.**
```

Fig. 5 Multiple alignments for BLBP. The homology between the sequences of *Gallus gallus* (NP_990639.1), *Salmo salar* (NP_001135371.1), *Xenopus laevis* (NP_001015907), *Homo sapiens* (NP_001437.1), *Rattus norvergicus* (NP_110459.1), and *Trachemys dorbignyi* (JQ356534) is higher than 65%.

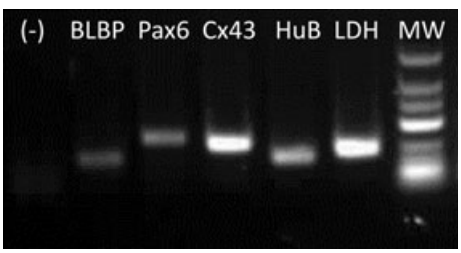

Fig. 6 Gel elctrophoresis of real-time RT-PCR products. A single band of the expected size was detected for all analyzed genes.

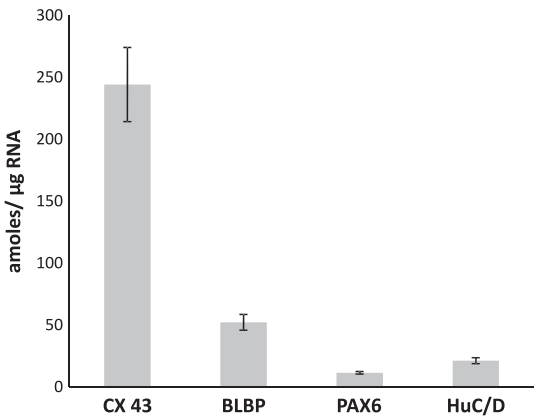

Fig. 7 Quantitative gene expression of control tissue. The bars represent the mean ($n = 3$) of absolute copy number (amoles) of each gene in 1 µg RNA. Data are represented as mean ± SEM.

performed but the spinal cord was not transected – was not significantly different to control animals ($n = 3$; $p > 0.2$; 4 days after sham injury; Figure S3). These results rule out an effect on the expression of these genes by the surgery itself.

Spatial profile of Hu, BLBP, and Cx43 expression

To test whether the changes in gene expression were accompanied by a change in the spatial profile of expression for the translated proteins, we did immunohistochemistry for Hu antigen, BLBP, and Cx43. Because our quantitative real-time PCR study did not reveal variations in PAX6 expression, immunohistochemistry for this transcription factor was not performed.

The expression pattern of Hu, BLBP, and Cx43 in the spinal cord of injured animals (4 and 12 days after lesion) and control animals is shown in Fig. 9. The monoclonal antibody HuC/D – which recognizes the three neuronal ribosome-associated Hu proteins HuB, HuC, and HuD (Marusich *et al.* 1994) – revealed that Hu was strongly expressed in the cell body around the nucleus of neurons in the gray matter, with a similar distribution within the gray

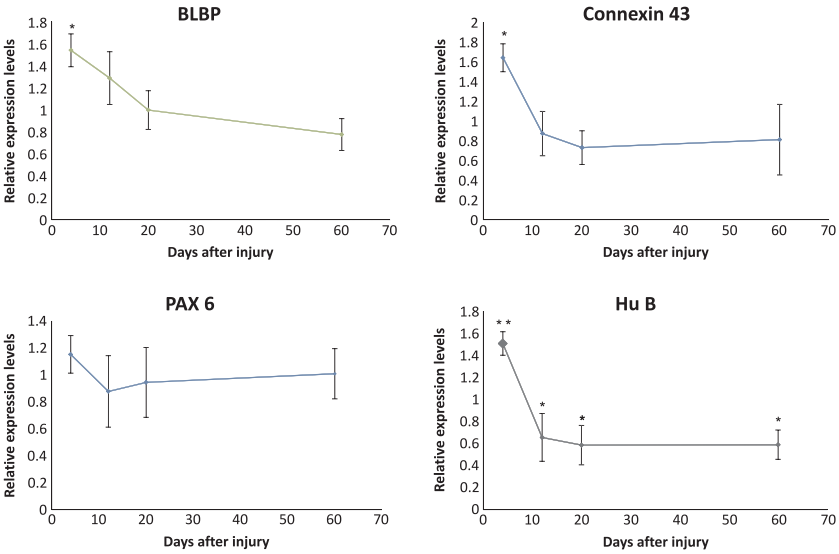

Fig. 8 Relative changes of mRNA expression of BLBP, HuB, Cx43, and Pax6 genes in injured tissue at different time points after spinal cord transection as compared with the values in control animals. Data are mean ± SEM ($n = 3$ for each time point). Significantly different from controls, $^{*}p < 0.05$; $^{**}p < 0.01$.

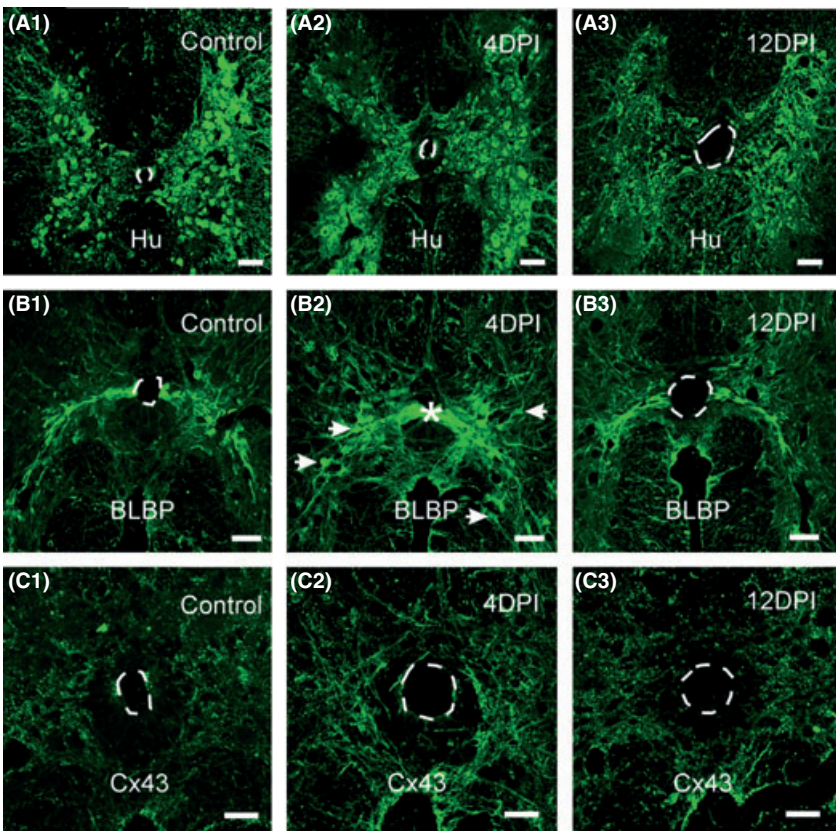

Fig. 9 Immunohistochemistry for Hu, brain lipid binding protein (BLBP) and connexin 43 in control tissue and the rostral stump of the regenerating spinal cord at 4 and 12 days post injury (DPI). A: Immunoreactivity for the Hu antigen in control (1) and after 4 DPI (2) and 12 DPI (3). B: BLBP expression in control (1) and at 4 DPI (2) and 12 DPI (3). The arrows indicate BLBP+ cells outside their common placements close to the CC; the asterisk in 2 indicates the collapsed lumen of the CC C: Expression of connexin 43 in control animals is shown in panel 1. The highest immunoreactivity was detected by day 4 (2) and reached normal levels by day 12 (3). Punctae quantification showed more particles at this time point when compared with control (see Figure S3). Calibration bars: 25 μm.

matter in control (Fig. 9A1) and injured (Fig. 9A2 and A3) animals.

The spatial profile of BLBP expression was also similar in normal (Fig. 9B1) and injured (Fig. 9B2 and B3) animals, with most BLBP+ cells located on the lateral aspects of the CC (Fig. 9B1–3). However, at 4 days after injury many BLBP+ cells were observed outside this region (Fig. 9B2, arrows).

Cx43 immunohistochemistry revealed punctae distributed widely in the white and gray matter of normal and injured spinal cords (Fig. 9C1–3). In line with the increased gene expression, the highest levels of Cx43 immunoreactivity

were observed at 4 DPI. (Fig. 9C2). Although 12 days after injury the Cx43 immunoreactivity decayed (Fig. 9C3), the number of punctae was still higher than control (Figure S4).

Because reactive astrogliosis may partly account for the increased expression of Cx43 around the CC, we did immunohistochemistry for GFAP in control and injured animals (4 DPI). Although the ependyma remained negative for GFAP, the expression of this protein in the region surrounding the CC seemed up-regulated at 4 DPI (Figure S5A). In line with these findings, the expression of the GFAP gene at 4 DPI was significantly increased compared with uninjured animals (Figure S5B).

Discussion

Turtles are amniote vertebrates that – unlike mammals – are able of a substantial degree of endogenous repair, probably because they retained multi-potent progenitor cells around the CC (Trujillo-Cenóz *et al.* 2007; Russo *et al.* 2008; Rehermann *et al.* 2009, 2011). Understanding the molecular mechanisms involved in injury induced plasticity in new model systems with efficient self-repair mechanisms may give important clues for the design of new therapies for treatment of spinal cord diseases (Tanaka and Ferretti 2009). A disadvantage of the turtle spinal cord as a model system to study regeneration is that no genomic resources from chelonians are available. In the present study, we used a cloning and sequencing strategy through gene amplification by degenerated primers design and described the partial sequences of genes that our previous studies pointed as potentially important for spinal cord regeneration in turtles (Rehermann *et al.* 2009). Surprisingly, our data show a high level of conservation of the analyzed genes among evolutionary distant organisms, validating the strategy and the biological model used in this study.

The analysis of mRNA expression changes after spinal cord transection has been a valuable approach to elucidate the underlying mechanisms of neural repair (Wu *et al.* 2005; Fujiyoshi *et al.* 2010; Arocho *et al.* 2011; Kuo *et al.* 2011; Nash *et al.* 2011). A key difference between spinal cord self-repair capabilities between mammals and turtles may be related with the persistence of progenitors functionally clustered via Cx43 and with a molecular phenotype characterized by the expression of BLBP and Pax6 (Russo *et al.* 2008). By applying quantitative RT-PCR – a highly sensitive technique allowing the quantification of small changes in gene expression (Wu *et al.* 2005) – we found that BLBP and Cx43 gene expression increased transiently, whereas Pax6 remained unchanged.

The increase in Cx43 mRNA expression induced by injury in our study resembles the elevation in Cx43 expression after a complete transection of the spinal cord of the rat as evaluated by *in situ* hybridization (Lee *et al.* 2005). Unlike the transient increase observed in turtles, Cx43 up-regulation in the rat increases progressively up to 4 weeks (Lee *et al.* 2005). The role played by Cx43 in response to injury of the nervous system is controversial, with some reports suggesting that increased levels are detrimental (Frantseva *et al.* 2002a,b), whereas others claim that Cx43 down-regulation results in an expansion in the lesion size (Siushansian *et al.* 2001; Nakase *et al.* 2004). The interference with Cx43 function after spinal cord injury reduces the reactive astrogliosis and neuronal death (O'Carroll *et al.* 2008) and improves functional recovery (Cronin *et al.* 2008). Our findings suggest that in turtles, the rapid decline of the initial up-regulation of Cx43 may minimize the detrimental effects of Cx43 mentioned above, possibly by avoiding the spread of injury.

It is not clear whether the increased expression of Cx43 reported here results in an increased number of hemichannels or functional gap junctions. Hemichannels have been postulated to mediate a component of ATP release (Garré *et al.* 2010) that acts on P2X7 channels during spinal cord injury (Peng *et al.* 2009). A role for hemichannels in early stages of spinal cord injury is suggested by the fact that low concentrations of a Cx43 mimetic peptide reduce hemichannel opening and prevent neuronal loss (O'Carroll *et al.* 2008).

The increased number of Cx43 punctae both in the white and gray matter suggests that the enhancement of Cx43 mRNA in the turtle spinal cord may be accounted by reactive astrocytes, as suggested by the increased expression of GFAP close to the CC at 4 DPI (see Figure S5). Although it is a reasonable assumption that Cx43 mRNA in CC-contacting progenitors is increased, a lack of variation or even a decreased expression in these cells could be masked by the over-expression in astrocytes. Single cell RT-PCR would be necessary to test whether CC-contacting progenitors react to injury by increasing Cx43 gene expression. In addition, given the role of electrical coupling in regulating the biology of progenitor cells (Duval *et al.* 2002; Bruzzone and Dermietzel 2006), it will be also important to test whether the changes in Cx43 mRNA match an increased electrical and metabolic coupling among BLBP/Pax6 progenitors.

The increased expression of BLBP seems to be an evolutionary preserved reaction to spinal injury because it is observed in salamanders (Monaghan *et al.* 2007), turtles (Rehermann *et al.* 2009 and this study), and mammals (White *et al.* 2010). In mammals, BLBP is not expressed in ependymal cells under normal conditions, but is transiently re-expressed after spinal cord injury (White *et al.* 2010). This suggests that when challenged, some cells in the mammalian ependyma are transformed into a phenotype of progenitors observed in the normal cord of turtles (Russo *et al.* 2008). BLBP expression in the ependyma of the mammalian cord returns to control levels 7 days after injury (White *et al.* 2010), paralleling the time course of the increased BLBP

mRNA in the turtle spinal cord. In mammals, however, the expression of BLBP continues in cells that co-express GFAP in the spared white matter and the lesion border, suggesting these cells are progenitors generating reactive astrocytes (White *et al.* 2010). Although BLBP+/GFAP+ cells are components of the cellular bridge that reconnects the severed spinal cord in turtles, they do not form a scar but provide a scaffold for regenerating axons (Rehermann *et al.* 2009). Thus, although BLBP signaling in mammals and turtles seem to share some common features, it is possible that the expression of BLBP after injury in turtles is linked to more adaptive mechanisms. The actual function of BLBP during repair is still unknown. BLBP belongs to the family of fatty acid binding proteins that regulate various metabolic processes and ligand trafficking in the CNS (Feng *et al.* 1994; Haunerland and Spener 2004). Interestingly, lipid turnover has been associated with axonal growth and nerve regeneration (Vance *et al.* 2010).

Our immunocytochemical study showed a tissue cytoarchitecture within the spinal cord stumps resembling that of the uninjured spinal cord, with BLBP+ progenitors still restricted to the lateral aspects of the CC. However, after injury there were BLBP+ cells at some distance from the CC raising the possibility they may have detached from the main clusters of progenitors. The migration of ependymal cells to the injury site has been shown in the spinal cord of rats (Mothe and Tator 2005) and mice (Meletis *et al.* 2008). However, the factors driving the migration of these cells to the injured zone are not clear. Reelin is up-regulated in the injured adult brain and has been proposed to drive subventricular progenitor cells away from the rostral migratory stream toward the lesion site (Courtès *et al.* 2011). The stromal cell derived factor-1 has been also proposed to attract ependymal cells and macrophages to the injury site (Tysseling *et al.* 2011). It remains to be demonstrated whether BLBP progenitors respond to these signals and migrate to the cellular bridge filling the gap between stumps (Rehermann *et al.* 2009).

Unlike the other genes explored in this study, Pax6 expression did not change significantly after injury. This is in striking contrast with the situation reported for the mammalian spinal cord in which Pax6 is not expressed in ependymal cells of the normal adult spinal cord but is transiently expressed in vimentin+/nestin+ ependymal cells after spinal cord injury (Yamamoto *et al.* 2001). The transcription factor Pax6 has been shown to regulate the proliferation of progenitors (Maekawa *et al.* 2005; Buffo 2007) and is a key neurogenic determinant both during development and in adult neurogenic niches (Kohwi *et al.* 2005; Bel-Vialar *et al.* 2007). The fact that BLBP up-regulation is not paralleled with an increase in Pax6 may imply that in the turtle, the progenitors are biased to generate glial cells during the initial stages of repair. This possibility is in line with our previous studies showing that newly generated cells express glial but not neuronal markers during spinal cord regeneration in the turtle (Rehermann *et al.* 2009). In amphibians and fishes, however, the mechanisms for endogenous repair include the generation of new neurons (Benraiss *et al.* 1999; Reimer *et al.* 2008; Tanaka and Ferretti 2009). Thus, although turtles are able to achieve some degree of functional regeneration after spinal cord injury, the reaction of the cord in terms of the generated cell lineages is more similar to mammals (Meletis *et al.* 2008) than to other low vertebrates. It has been proposed that the inability for neurogenesis after injury in the mammalian cortex arise from the antagonism of the pro-neural factor Pax6 by Olig2 (Buffo 2007). It remains to be explored the contribution of other transcription factors to set the lineage potential of progenitors after injury in the turtle spinal cord.

Hu expression exhibited a slight up-regulation 4 days after injury to reach half its normal expression levels at 12, 20, and 60 days post injury. The Hu family of neuronal proteins (HuB, HuC and HuD) exhibit a high degree of sequence homology (Okano and Darnell 1997) playing important roles in neuronal differentiation and plasticity by affecting post-transcriptional aspects of RNA metabolism (Hinman and Lou 2008). For example, over-expression of HuD increases the neurite outgrowth (Anderson *et al.* 2000, 2001) and knockdown of HuC results in impaired spatial learning in mice (Quattrone *et al.* 2001). The increase in HuB mRNA after spinal cord injury in turtles is because of up-regulation of gene expression in pre-existent neurons because our previous studies did not show evidence of neurogenesis induced by injury (Rehermann *et al.* 2011). Because Hu proteins are important to stabilize target mRNAs, it is possible that the increased Hu transcription is a homeostatic adjustment to spare neuronal elements challenged by the insult. Although Hu proteins have been shown to be transiently over-expressed after injury of peripheral nerves (Anderson *et al.* 2003), their role in healing is not clear. The late reduction in Hu mRNA levels may reflect the loss of neurons in the stumps. In mammals (Profyris *et al.* 2004) and in salamander (Monaghan *et al.* 2007), neuronal-related genes also appeared down-regulated after injury. In the rat, the decline in the expression of neural-specific transcripts is accompanied by a significant rise in tissue repairing genes that are remarkably similar to those acting in dermal wound healing (Velardo *et al.* 2004).

The time course of the change in gene expression implies that the genes selected in this study participate mostly of the early response to injury. It is noteworthy that at this time, the bridge linking the rostral and caudal stumps is not fully developed yet, and from a functional point of view, motor activity is only limited to segmental spinal reflex movements as stepping patterns appear no less than 60 days after injury (Rehermann *et al.* 2009). This implies that the endogenous repair mechanisms involve a more complex set of genes turning on and off at different stages of repair. Future studies should explore the genes involved in later stages of regeneration of the turtle spinal cord leading to some degree of functional recovery.

Concluding, our study shows that molecular and bioinformatics tools can be used to associate gene expression changes with cellular and functional aspects of spinal cord regeneration. The high conservation degree found for the selected genes in this study validates our biological model and illustrates the utility of *T. dorbignyi* for identifying the genes and gene functions that sustain the remarkable self-repair mechanisms within the spinal cord of some vertebrates.

Acknowledgments

We thank M.I. Rehermann for technical assistance and Dr. J Sáez for the generous gift of the antibody against connexin 43. The work described here was supported by Grant # FCE_2920 from ANII and Grant Number R01NS048255 from the National Institute of Neurological Disorders and Stroke to R.E.R. The content is solely the responsibility of the authors and does not necessarily represent the official views of the National Institute of Neurological Disorders and Stroke or the National Institutes of Health. The authors declare no conflicts of interest.

GG, GL, CR, OTC, and RER contributed to the conception and design of the experimental approach; GG, GL, and CR acquired, analyzed, and interpreted data; GG and RER drafted the paper; all authors revised the paper for important intellectual content and approved the final version of the manuscript.

Supporting information

Additional supporting information may be found in the online version of this article.

Figure S1. Bioanalyzer electrophoresis.

Figure S2. Standard curve for Connexin 43.

Figure S3. Relative changes of mRNA expression for Cx43, BLBP, Pax6, and HuB genes 4 days after a sham injury as compared with values in control animals.

Figure S4. Quantification of Cx43 punctae in the normal and injured cord.

Figure S5. Expression of GFAP in control and 4 DPI animals.

As a service to our authors and readers, this journal provides supporting information supplied by the authors. Such materials are peer-reviewed and may be re-organized for online delivery, but are not copy-edited or typeset. Technical support issues arising from supporting information (other than missing files) should be addressed to the authors.

References

Anderson K. D., Morin M. A., Beckel-Mitchener A., Mobarak C. D., Neve R. L., Furneaux H. M., Burry R. and Perrone-Bizzozero N. I. (2000) Overexpression of HuD, but not of its truncated form HuD I+II, promotes GAP-43 gene expression and neurite outgrowth in PC12 cells in the absence of nerve growth factor. *J. Neurochem.* **75**, 1103–1114.

Anderson K. D., Sengupta J., Morin M., Neve R. L., Valenzuela C. F. and Perrone-Bizzozero N. I. (2001) Overexpression of HuD accelerates neurite outgrowth and increases GAP-43 mRNA expression in cortical neurons and retinoic acid-induced embryonic stem cells in vitro. *Exp. Neurol.* **168**, 250–258.

Anderson K. D., Merhege M. A., Morin M., Bolognani F. and Perrone-Bizzozero N. I. (2003) Increased expression and localization of the RNA-binding protein HuD and GAP-43 mRNA to cytoplasmic granules in DRG neurons during nerve regeneration. *Exp. Neurol.* **183**, 100–108.

Anton E.S., Marchionni M. A., Lee K. F. and Rakic P. (1997) Role of GGF/neuregulin signaling in interactions between migrating neurons and radial glia in the developing cerebral cortex. *Development* **124**, 3501–3510.

Arocho L. C., Figueroa J. D., Torrado A. I., Santiago J. M., Vera A. E. and Miranda J. D. (2011) Expression profile and role of EphrinA1 Ligand after spinal cord injury. *Cell. Mol. Neurobiol.* **31**, 1057–1069.

Bel-Vialar S., Medevielle F. and Pituello F. (2007) The on/off of Pax6 controls the tempo of neuronal differentiation in the developing spinal cord. *Dev. Biol.* **305**, 659–673.

Benraiss A., Arsanto J. P., Coulon J. and Thouveny Y. (1999) Neurogenesis during caudal spinal cord regeneration in adult newts. *Dev. Genes. Evol.* **209**, 363–369.

Bruzzone R. and Dermietzel R. (2006) Structure and function of gap junctions in the developing brain. *Cell Tissue Res.* **326**, 239–248.

Buffo A. (2007) Fate determinant expression in the lesioned brain: Olig2 induction and its implications for neuronal repair. *Neurodegener. Dis.* **4**, 328–332.

Cheng A., Tang H., Cai J., Zhu M., Zhang X., Rao M. and Mattson M. P. (2004) Gap junctional communication is required to maintain mouse cortical neural progenitor cells in a proliferative state. *Dev. Biol.* **272**, 203–216.

Courtès S., Vernerey J., Pujadas L., Magalon K., Cremer H., Soriano E., Durbec P. and Cayre M. (2011) Reelin controls progenitor cell migration in the healthy and pathological adult mouse brain. *PLoS ONE* **6**, e20430.

Cronin M., Anderson P. N., Cook J. E., Green C. R. and Becker D. L. (2008) Blocking connexin43 expression reduces inflammation and improves functional recovery after spinal cord injury. *Mol. Cell. Neurosci.* **39**, 152–160.

Duval N., Gomes D., Calaora V., Calabrese A., Meda P. and Bruzzone R. (2002) Cell coupling and Cx43 expression in embryonic mouse neural progenitor cells. *J. Cell Sci.* **115**, 3241–3251.

Feng L., Hatten M. E. and Heintz N. (1994) Brain lipid-binding protein (BLBP): a novel signaling system in the developing mammalian CNS. *Neuron* **12**, 895–908.

Frantseva M. V., Kokarovtseva L., Naus C. G., Carlen P. L., MacFabe D. and Perez Velazquez J. L. (2002a) Specific gap junctions enhance the neuronal vulnerability to brain traumatic injury. *J. Neurosci.* **22**, 644–653.

Frantseva M. V., Kokarovtseva L. and Perez Velazquez J. L. (2002b) Ischemia-induced brain damage depends on specific gap-junctional coupling. *J. Cereb. Blood Flow Metab.* **22**, 453–62.

Fujiyoshi T., Kubo T., Chan C. C., Koda M., Okawa A., Takahashi K. and Yamazaki M. (2010) Interferon-γ decreases chondroitin sulfate proteoglycan expression and enhances hindlimb function after spinal cord injury in mice. *J.Neurotrauma* **27**, 2283–94.

Garré J. M., Retamal M. A., Cassina P., Barbeito L., Bukauskas F. F., Sáez J. C., Bennett M. V. and Abudara V. (2010) FGF-1 induces ATP release from spinal astrocytes in culture and opens pannexin and connexinhemichannels. *PNAS* **107**, 22659–22664.

Haunerland N. H. and Spener F. (2004) Fatty acid-binding proteins-insights from genetic manipulations. *Prog. Lipid Res.* **43**, 328–349.

Heins N., Malatesta P., Cecconi F., Nakafuku M., Tucker K. L., Hack M. A., Chapouton P., Barde Y. A. and Götz M. (2002) Glial cells

generate neurons: the role of the transcription factor Pax6. *Nat. Neurosci.* **5**, 308–315.

Hinman M. N. and Lou H. (2008) Diverse molecular functions of Hu proteins. *Cell. Mol. Life Sci.* **65**, 3168–3181.

Kohwi M., Osumi N., Rubenstein J. L. and Alvarez-Buylla A. (2005) Pax6 is required for making specific subpopulations of granule and periglomerularneurons in the olfactory bulb. *J. Neurosci.* **25**, 6997–7003.

Kuo H. S., Tsai M. J., Huang M. C., Chiu C. W., Tsai C. Y., Lee M. J., Huang W. C., Lin Y. L., Kuo W. C. and Cheng H. (2011) Acid fibroblast growth factor and peripheral nerve grafts regulate Th2 cytokine expression, macrophage activation, polyamine synthesis, and neurotrophin expression in transected rat spinal cords. *J. Neurosci.* **31**, 4137–4147.

Lee S. K. and Pfaff S. L. (2001) Transcriptional networks regulating neuronal identity in the developing spinal cord. *Nat. Neurosci.* **4**, 1183–1191.

Lee I. H., Lindqvist E., Kiehn O., Widenfalk J. and Olson L. (2005) Glial and neuronal connexin expression patterns in the rat spinal cord during development and following injury. *J. Comp. Neurol.* **489**, 1–10.

Maekawa M., Takashima N., Arai Y., Nomura T., Inokuchi K., Yuasa S. and Osumi N. (2005) Pax6 is required for production and maintenance of progenitor cells in postnatal hippocampal neurogenesis. *Genes Cells* **10**, 1001–1014.

Marusich M. F., Furneaux H. M., Henion P. D. and Weston J. A. (1994) Hu neuronal proteins are expressed in proliferating neurogenic cells. *J. Neurobiol.* **25**, 143–155.

Meletis K., Barnabé-Heider F., Carlen M., Evergren E., Tomilin N., Shupliakov O. and Frisén J. (2008) Spinal cord injury reveals multilineage differentiation of ependymal cells. *PLoS Biol.* **6**, e182.

Monaghan J. R., Walker J. A., Page R. B., Putta S., Beachy C. K. and Voss S. R. (2007) Early gene expression during natural spinal cord regeneration in the salamander Ambystomamexicanum. *J. Neurochem.* **101**, 27–40.

Mothe A. J. and Tator C. H. (2005) Proliferation, migration, and differentiation of endogenous ependymal region stem/progenitor cells following minimal spinal cord injury in the adult rat. *Neuroscience* **131**, 177–187.

Mountcastle V.B. (1980). Effects of spinal transection, in: *Medical physiology VI* (Mountcastle V. B., ed), pp. 781–785. CV Mosby Company, St. Louis, MO, USA.

Nakase T., Söhl G., Theis M., Willecke K. and Naus C. C. (2004) Increased apoptosis and inflammation after focal brain ischemia in mice lacking connexin43 in astrocytes. *Am. J. Pathol.* **164**, 2067–2075.

Nash B., Thomson C. E., Linington C., Arthur A. T., McClure J. D., McBride M. W. and Barnett S. C. (2011) Functional duality of astrocytes in myelination. *J. Neurosci.* **31**, 13028–13038.

O'Carroll S. J., Alkadhi M., Nicholson L. F. and Green C. R. (2008) Connexin 43 mimetic peptides reduce swelling, astrogliosis, and neuronal cell death after spinal cord injury. *Cell. Commun. Adhes.* **15**, 27–42.

Okano H. J. and Darnell R. B. (1997) A hierarchy of Hu RNA binding proteins in developing and adult neurons. *J. Neurosci.* **17**, 3024–3037.

Parker T. J. and Harwell W. A. (1949) *A text-book of zoology*. MacMillan and Co., London.

Peng W., Cotrina M. L., Han X., Yu H., Bekar L., Blum L., Takano T., Tian G. F., Goldman S. A. and Nedergaard M. (2009) Systemic administration of an antagonist of the ATP-sensitive receptor P2X7 improves recovery after spinal cord injury. *PNAS* **106**, 12489–12493.

Pinto L. and Götz M. (2007) Radial glial cell heterogeneity—the source of diverse progeny in the CNS. *Prog. Neurobiol.* **83**, 2–23.

Profyris C., Cheema S. S., Zang D., Azari M. F., Boyle K. and Petratos S. (2004) Degenerative and regenerative mechanisms governing spinal cord injury. *Neurobiol. Dis.* **15**, 415–436.

Quattrone A., Pascale A., Nogues X., Zhao W., Gusev P., Pacini A. and Alkon D. L. (2001) Posttranscriptional regulation of gene expression in learning by the neuronal ELAV-like mRNA-stabilizing proteins. *PNAS* **98**, 11668–11673.

Rehermann M. I., Marichal N., Russo R. E. and Trujillo-Cenóz O. (2009) Neural reconnection in the transected spinal cord of the freshwater turtle *Trachemys dorbignyi*. *J. Comp. Neurol.* **515**, 197–214.

Rehermann M. I., Santiñaque F., López-Carro B., Russo R. E. and Trujillo-Cenóz O. (2011) Cell proliferation and cytoarchitectural remodeling during spinal cord reconnection in the fresh-water turtle *Trachemys dorbignyi*. *Cell Tissue Res.* **344**, 415–433.

Reimer M. M., Sörensen I., Kuscha V., Frank R. E., Liu C., Becker C. and Becker T. (2008) Motor neuron regeneration in adult zebrafish. *J. Neurosci.* **28**, 8510–8516.

Russo R. E., Reali C., Radmilovich M., Fernández A. and Trujillo-Cenóz O. (2008) Connexin 43 delimits functional domains of neurogenic precursors in the spinal cord. *J. Neurosci.* **28**, 3298–3309.

Siushansian R., Bechberger J. F., Cechetto D. F., Hachinski V. C. and Naus C. C. (2001) Connexin43 null mutation increases infarct size after stroke. *J Comp Neurol.* **440**, 387–394.

Stensaas L. J. (1983) Regeneration in the spinal cord of the newt Notopthalmus (Triturus) pyrrhogaster, in *Spinal cord reconstruction* (Kao C.C., Bunge R.P. and Reier P.J., eds), pp. 121–149. Raven, New York.

Tanaka E. M. and Ferretti P. (2009) Considering the evolution of regeneration in the central nervous system. *Nat. Rev. Neurosci.* **10**, 713–723.

Thuret S., Moon L. D. and Gage F. H. (2006) Therapeutic interventions after spinal cord injury. *Nat. Rev. Neurosci.* **7**, 628–643.

Trujillo-Cenóz O., Fernández A., Radmilovich M., Reali C. and Russo R. E. (2007) Cytological organization of the central gelatinosa in the turtle spinal cord. *J. Comp. Neurol.* **502**, 291–308.

Tysseling V.M., Mithal D., Sahni V., Birch D., Jung H., Belmadani A., Miller R.J. and Kessler J.A. (2011) SDF1 in the dorsal corticospinal tract promotes CXCR4 + cell migration after spinal cord injury. *J. Neuroinflammation.* **8**, 16.

Vance J. A., Campenot R. B. and Vance D. E. (2010) The synthesis and transport of lipids for axonal growth and nerve regeneration. *Biochim. Biophys. Acta* **1486**, 84–96.

Velardo M. J., Burger C., Williams P. R., Baker H. V., López M. C., Mareci T. H., White T. E., Muzyczka N. and Reier P. J. (2004) Patterns of Gene Expression Reveal a Temporally Orchestrated Wound Healing Response in the Injured Spinal Cord. *J. Neurosci.* **24**, 8562–8576.

White R. E., McTigue D. M. and Jakeman L. B. (2010) Regional heterogeneity in astrocyte responses following contusive spinal cord injury in mice. *J. Comp. Neurol.* **518**, 1370–1390.

Wu X., Yoo S. and Wrathall J. R. (2005) Real-time quantitative PCR analysis of temporal–spatial alterations in gene expression after spinal cord contusion. *J. Neurochem.* **93**, 943–952.

Yamamoto S., Nagao M., Sugimori M. *et al.* (2001) Transcription factor expression and Notchdependent regulation of neural progenitors in the adult rat spinal cord. *J. Neurosci.* **21**, 9814–9823.